Paper:
Jalali, H., Khodaparast, H., Madinei, H. & Friswell, M. (2019). Stochastic modelling and updating of a joint contact interface. *Mechanical Systems and Signal Processing, 129*, 645-658.
http://dx.doi.org/10.1016/j.ymssp.2019.04.003

Stochastic Modelling and Updating of a Joint Contact Interface

H. Jalali[1], H. Haddad Khodaparast[1], H. Madinei[1], M. I. Friswell[1]
[1] Swansea University, College of Engineering, Bay Campus, Fabian Way, Crymlyn Burrows, Swansea, SA1 8EN, United Kingdom

Abstract

Dynamic properties of the contact interfaces in joints and mechanical connections have a great influence on the overall dynamic properties of assembled structures. Uncertainty and nonlinearity are two major effects of contact interfaces which introduce challenges in accurate modeling. Randomness in surface roughness quality, surface finish and contact preload are the main sources of variability in the contact interfaces. On the other side, slip and slap are two mechanisms responsible for nonlinear behavior of joints. Stochastic linear/nonlinear models need to be developed for such uncertain structures to be used in dynamic response analysis or system parameter identification. In this paper, variability in linear behavior of an assembled structure containing a bolted lap-joint is investigated by using experimental results. A stochastic model is then constructed for the structure by employing a stochastic generic joint model and the uncertainty in the joint model parameters is identified by using a Bayesian identification approach.

Introduction

The aim of using joints and fasteners in many engineering structures is to transfer forces and moments between different substructures through frictional contact interfaces. Due to the lack of information about the various parameters- such as contact stiffness and damping, surface roughness quality, preload etc.- frictional contact interfaces introduce uncertainty in the dynamic properties of assembled structures. Measurement, quantification and modelling of this uncertainty is a step forward in engineering structural design. Since deterministic modeling and identification do not provide promising results for assembled structures, stochastic modeling and uncertainty quantification approaches should be developed.

Contact interfaces are among the main sources of uncertainty in assembled structures [1]. There are principally two classes of uncertainty in joints. The first, and most important, class of uncertainty arises from the deformation of asperities and the consequent relaxation of the joint [2], for example there can be as much variation as ±30% of the expected tension in a bolt when using the torque tightening method and bolt tension can drop by more than 40% over a short period of exposure to vibration. Also there are cases when bolt tension can increase rather than decrease depending upon the excitation frequency and vibration level. Bolt tension generally reduces quickly just after tightening. The second type of uncertainty in joints is due to the assembly process and the accumulation of engineering tolerances.

Variability in contact interface parameters due to the deformation of asperities can be attributed to the randomness in the preload and contact surface characteristics such as surface finish (or roughness quality). Variability and repeatability in the dynamic response of assembled structures have been studied by Brake *et.al.* [3]. Gangadharan et al. [4] identified the stochastic welded joint model parameter in a car body by employing two coupled and uncoupled models. Lopez et al. [5] considered the connection between two substructures of a space structure as random springs and investigated the uncertainty in structural responses such as FRFs due to the uncertainty in joint parameters. Guo and Zhang [6] identified the uncertainty in joint model parameters by using updating approaches. Castelluccio and Brake [7] employed FE simulation to investigate the model input and form uncertainties in threaded fasteners. They characterized the source of uncertainty and variability in modelling fasteners as uncertainty in geometry, materials, mechanics and methodology.

Stochastic model updating methods can be generally categorized into two groups. These are probabilistic and non-probabilistic methods. Non-probabilistic methods include interval updating e.g. [8] [9] [10] and fuzzy model updating e.g. [11] [12] [13], while perturbation methods such as [14] [15] [16] [17] and Bayesian updating [18] [19] [20] are examples of the probabilistic methods. Govers et al. [21] compared the interval updating methods with perturbation methods and concluded that interval model updating is more conservative than perturbation methods although in the case of limited data the interval approach seems to be more suitable because it does not involve any probabilistic assumption. The review paper by Simoen [22] and references therein show the considerable attention that has already been paid to the subject of non-deterministic model updating. Recently there has been great attention on the use of Bayesian model updating in the context of stochastic model updating. The choice of likelihood functions is often assumed to have a normal distribution while the validity of this assumption cannot be readily assessed.

In this paper stochastic modeling and uncertainty quantification of the contact interface of a bolted lap-joint is considered. First, two sets of beam substructures are provided and are combined to build a set of nominally identical assembled structures. Experimental modal testing is employed to study the effects of preload and surface roughness quality on the variability of modal parameters of the assembled beam structures. Then, a stochastic dynamic model capable of regenerating the experimental modal properties is constructed by introducing a new stochastic joint model. Finally, the Bayesian approach is adopted to identify the stochastic joint parameters by employing the stochastic model of the experimental modal properties. A new likelihood function is introduced and employed in this paper which does not rely on the assumption of a Normal distribution for the error function which is a key assumption in stochastic model updating.

Experimental analysis of the bolted structures

To check the effects of randomness in contact surface roughness parameters on the variability of the dynamic characteristics of assembled structures, i.e. natural frequencies and damping ratios, 25 nominally identical bolted beam structures are prepared. The beam structures are identical in dimensional and material properties and it is assumed that there is a variability between their contact surface parameters such as their contact surface profiles. The dimensions of the test structures are shown in Figure 1. The test structures, which are made from steel, have the material properties $E = 208$ GPa and $\rho = 7860$ kg/m^3.

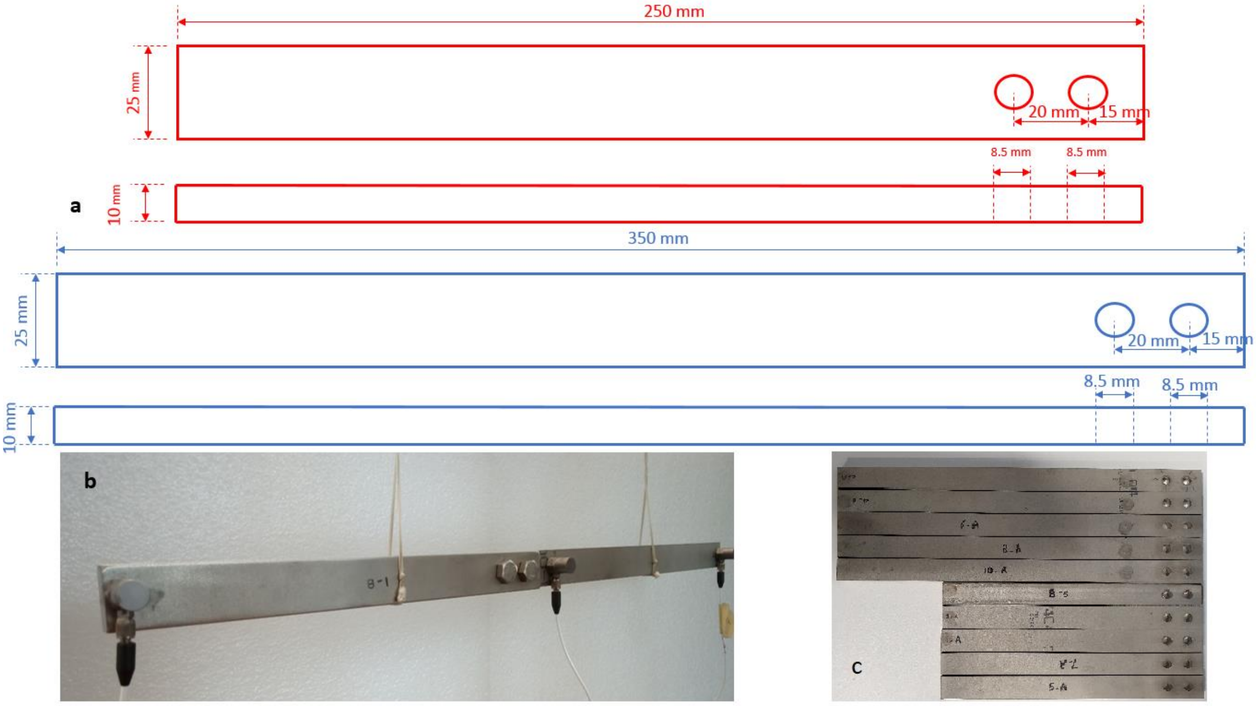

Figure 1. The test structures: (a) dimensions of the substructures, (b) test set-up of the assembled structures, (c) samples of the substructures

Joints have a great influence on the dynamic properties of assembled structures. In fact, the local flexibility and damping introduced by joints changes the overall dynamic response of the structures [23]. The equivalent stiffness and damping characteristics of the contact interfaces of the joints is a function of contact surface parameters such as surface roughness and preload [24] [25] [26]. Therefore small variability in the contact surface parameters results in significant effects on the overall dynamic characteristics. In this paper, experimental modal testing is employed to investigate the effects of variability in the contact interface parameters on the variability of natural frequencies and damping ratios.

In the modal testing procedure, care has been taken to keep other types of uncertainties to a minimum. The beam substructures shown in Figure 1 are combined by using identical M8 bolts and nuts and nominally identical assembled structures are obtained. A KTC Digital Ratchet Torque Wrench model GEK030-C3 is used to tighten the bolts to a specific level. In this paper three torque levels are used, 7 Nm, 15 Nm and 23 Nm. To minimise the effects of uncertainty in boundary conditions, free-free boundary conditions are used for the assembled beam structures by suspending them using flexible strings as shown in Figure 1.

Hammer testing is employed in this paper and the amplitude of the applied forces to the structures is kept low to ensure that the structure behaves linearly. Three accelerometers are used to measure the response of the structures. Bolts and accelerometers mass characteristics change the natural frequencies of the assembled structures used in this paper in a range of frequencies which is comparable to the variation in the natural frequencies due to randomness in the contact interface. Therefore, a source of uncertainty in the test structures can be the variability in location and orientation of the bolts and accelerometers, which should be avoided in the test procedure. A unique arrangement of bolts, accelerometer locations and hammer impact point relative to the two substructures, as shown in Figure 2, is used in the modal testing of all assembled beam structures. This ensures the effects of unwanted uncertainty in the test results due to the test procedure are kept to a minimum level.

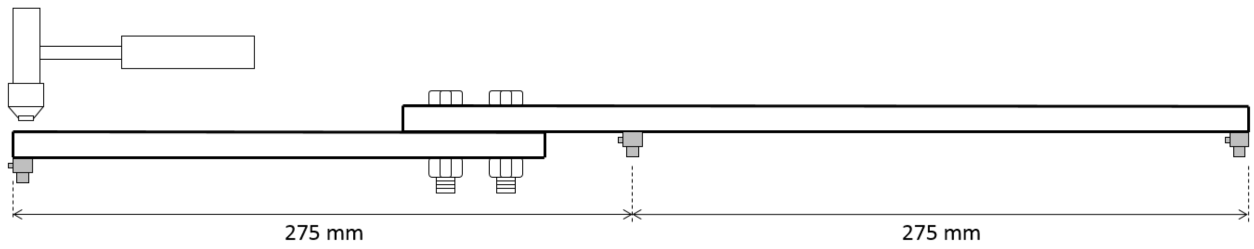

Figure 2. Arrangement for the modal testing

Experimental FRFs corresponding to different bolt tightening torque levels are shown in Figure 3.

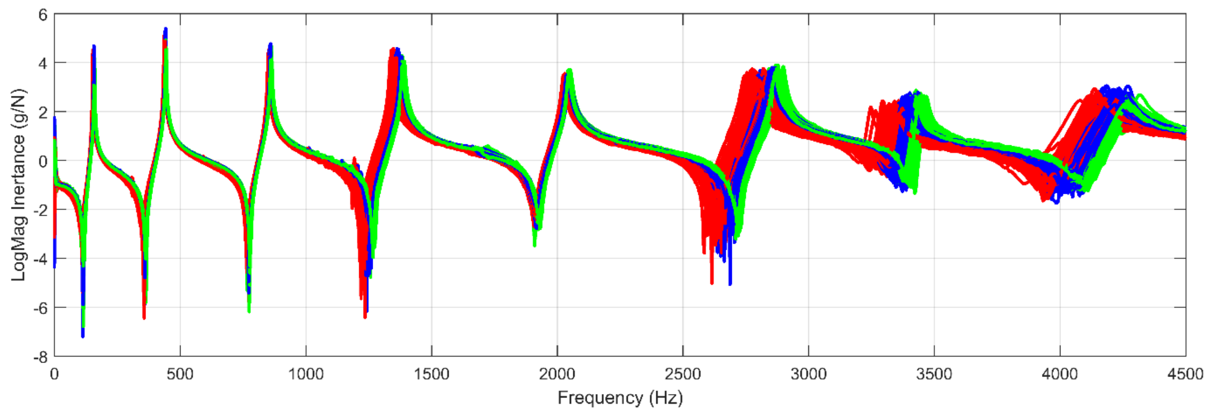

Figure 3. The FRFs corresponding to 7 Nm (red), 15 Nm (blue) and 23 Nm (green)

Figure 3 indicates that by increasing the contact interface preload (or bolt tightening torque) the natural frequencies increase. However, the change in the damping ratio is different for various modes and preloads. It is expected that there would be a bolt torque that maximises the damping ratios; for both low and high torque the dissipation would be low (if the joint is very stiff there is no micro-slip). It is worth noting that the mode shapes of the beam will affect the damping ratio as will be discussed in the last section of the paper, i.e. 'joint model damping parameter'. To quantitatively investigate the effects of preload and variability in the contact interface on modal properties, the peak-picking modal parameter estimation approach [27] is used to extract the modal properties of the assembled structures using the experimental results presented in Figure 3. Figures 4 and 5 show the variability in the natural frequencies and damping ratios for different modes.

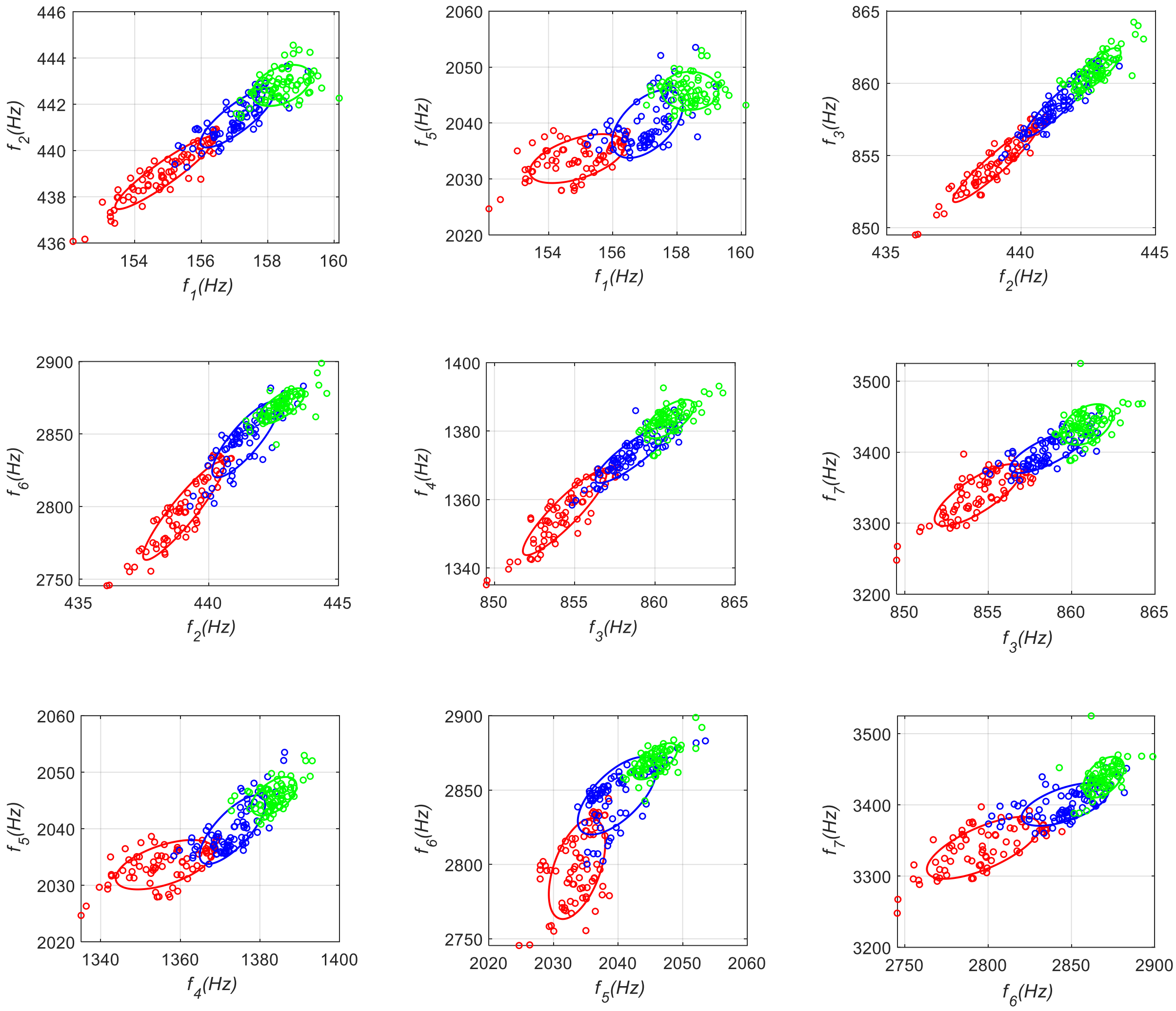

Figure 4. Variability in the natural frequencies: 7 Nm (red), 15 Nm (blue) and 23 Nm (green)

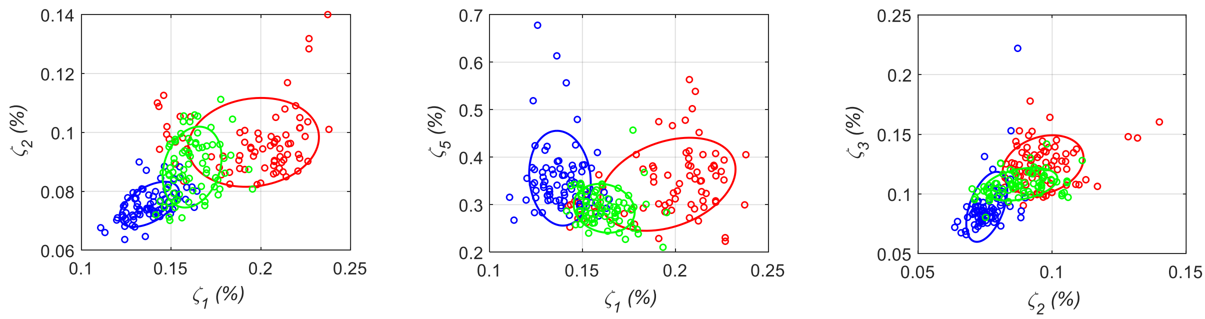

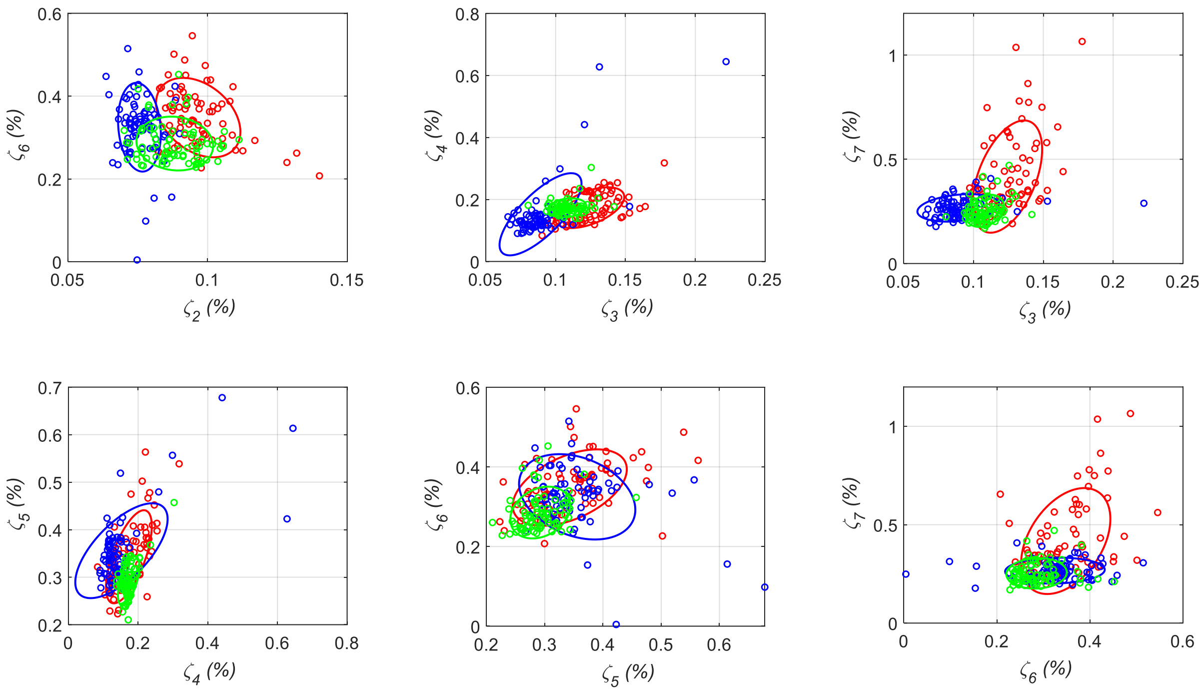

Figure 5. Variability in the damping ratios: 7 Nm (red), 15 Nm (blue) and 23 Nm (green)

The experimental results presented in Figures 4 and 5 show that there is significant variability in the natural frequencies and damping ratios. The results show that the variability reduces at higher preload. The lower modes are likely to be more correlated because they are likely to depend mainly on one of the equivalent joint parameters, whereas for higher modes other joint parameters could become important. Variability in the damping ratios is higher than for the natural frequencies and there is no clear relationship between variability in the damping ratios and preload, although the results indicate higher variability in the damping ratios for lower preload, which is expected. Another observation is that there doesn't appear to be any clear correlation between the different damping ratios, in contrast with frequencies shown in Figure 4 (especially the lower modes) where there are clear correlations. It is worth mentioning that since identification of damping is more sensitive to noise compared to the identification of natural frequencies, and all of the variability in the damping ratios shown in Figure 5 cannot be attributed to the randomness in the contact interface. The experimental results presented in this section are used in the next sections to construct an accurate stochastic dynamic model for the structure.

Mathematical modeling

There are two important steps in modeling mechanical structures: constructing an accurate model and improving its precision. An accurate model means a model which is potentially capable of representing the actual mechanical structure. Accurate modeling is not possible unless every single part of the actual structure is properly considered in its mathematical representation. Modeling mysterious and physically unknown sections such as joints is very important in constructing an accurate model for the structures. Having an accurate model, its precision can be improved by using experimental results and employing system identification approaches. Therefore, a precise model means a model which predicts the dynamic properties of an actual mechanical structure very closely. Without having an accurate model, approaching to a precise model is either impossible or is possible but results in a model with a poor physical justification, i.e. negative physical parameters such as stiffness coefficients. In fact, the model parameters may compensate for the inaccuracy in the modeling. Accurate modeling is even more important in stochastic structural modeling and identification. Compensation for the modeling inaccuracy results in erroneous distributions of the identified model parameters. Constructing accurate models capable of representing the variability in the dynamic properties of the contact interfaces in assembled structures is considered in this section.

Modeling an assembled structure containing a joint contact interface is considered by using offset-beam and stochastic generic-joint elements. The dynamic modeling discussed in this section will be used to identify the joint model parameters by using experimental results in the next sections. A bolted structure, as shown in Figure 6(a), is considered. The structure consists of two beam substructures connected through a frictional contact interface provided by a bolted lap joint.

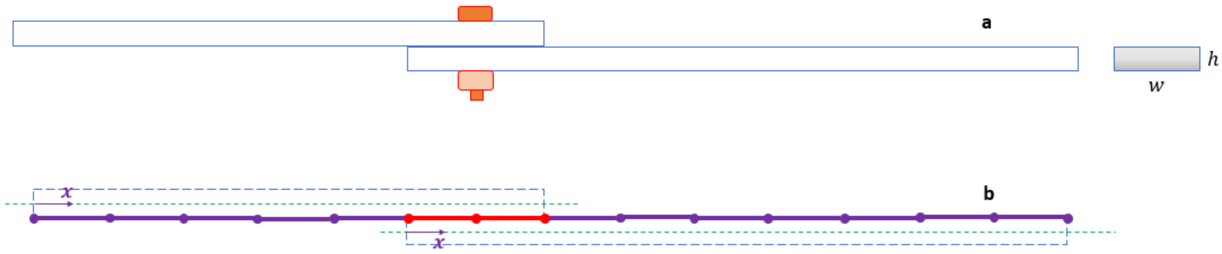

Figure 6. The joined structure: (a) schematic, (b) corresponding FE model

The structure can be divided into two beam sections and one joint section. The dynamic behaviour of the beam sections can be represented using different beam theories [28]. Beam sections can be represented by using analytical or FE models. The FE modeling approach is considered for the beam sections in this paper. Modeling the joint section has been considered by many researchers in the past and different linear [29] [30] [31] and nonlinear [32] [33] [23] [34] [35] [36] joint models have been proposed. In modeling the assembled structure shown in Figure 6(a), special care should be taken since the beam substructures are in contact in a region far from their centerlines at the joint section. This fact should be considered in the modeling, as described in the following.

The beam sections of the structure shown in Figure 6(a) are modelled using offset Timoshenko beam elements [37]. Usually in the FE method the nodes are located on center line of the beam elements. However, to be able to effectively assemble the FE model of the structure shown in Figure 6(a), the nodes should be placed at the bottom surface of the upper beam and the upper surface of the lower beam as shown in Figure (6b). By displacing the nodes, the stiffness matrix of the offset beam element is obtained as,

$$[K_b]=\begin{bmatrix} k_A & 0 & -k_A q & -k_A & 0 & k_A q \\ 0 & 12k_I & 6Lk_I & 0 & -12k_I & 6Lk_I \\ -k_A q & 6Lk_I & (4+\phi)L^2 k_I + k_A q^2 & k_A q & -6Lk_I & (2-\phi)L^2 k_I - k_A q^2 \\ -k_A & 0 & k_A q & k & 0 & k_A q \\ 0 & -12k_I & -6Lk_I & 0 & 12k_I & -6Lk_I \\ k_A q & 6Lk_I & (2-\phi)L^2 k_I - k_A q^2 & k_A q & -6Lk_I & (4+\phi)L^2 k_I + k_A q^2 \end{bmatrix} \quad (1)$$

where $q = h/2$ for the upper beam and $q = -h/2$ for the lower beam, $k_A = EA/L$ and $k_I = EI/(1+\phi)L^3$ and L is the length of the beam element. E, A and I are Young's modulus, area of the cross section and bending moment of inertia, respectively. $\phi = 12EI\alpha/GAL^2$ gives the relative importance of shear deformation to bending deformation. G is the shear modulus and α is the shear area coefficient. The effect of offsetting on the mass matrix is negligible and hence the mass effect of the beam sections of the structure is modeled by using the mass matrix of Timoshenko beam element (Appendix).

Next, modeling the joint section of the assembled structure shown in Figure 6(a) is considered. Due to the complexities that exist in the behaviour of the contact interface, there are no analytical equations governing the dynamic behaviour of the joint section and the joint section must be modeled using the FE approach. The joint section can be modeled by using generic joint elements [33]. To consider the randomness in the joint contact surfaces described in the previous sections, the joint model parameters may be considered as random fields to construct a stochastic joint model. Therefore, in this paper, the joint section is modelled by using 2-noded stochastic beam like generic elements [33]. In this regard, the stiffness matrix of the stochastic generic joint element is considered as,

$$[K_j]=\frac{1}{L^2}\begin{bmatrix} 2k_A & 0 & 0 & -2k_A & 0 & 0 \\ 0 & 4k_1(\theta) & 2Lk_1(\theta) & 0 & -4k_1(\theta) & 2Lk_1(\theta) \\ 0 & 2Lk_1(\theta) & L^2(k_1(\theta)+k_2(\theta)) & 0 & -2Lk_1(\theta) & L^2(k_1(\theta)-k_2(\theta)) \\ -2k_A & 0 & 0 & 2k_A & 0 & 0 \\ 0 & & -2Lk_1(\theta) & 0 & 4k_1(\theta) & -2Lk_1(\theta) \\ 0 & & L^2(k_1(\theta)-k_2(\theta)) & 0 & -2Lk_1(\theta) & L^2(k_1(\theta)+k_2(\theta)) \end{bmatrix} \tag{2}$$

where $k_i(\theta) = k_{i0}(1 + \bar{\varepsilon}_i f_i(\theta))$ $(i = 1,2)$. k_{i0} and $0 < \bar{\varepsilon}_i \ll 1$ (i=1,2) are the mean values and deterministic constants and $f_i(\theta)$ is a zero mean random field describing the variability in the stiffness parameters of the joint element. In equation (2), k_A is the axial stiffness of the beam structure and $k_1(\theta)$ and $k_2(\theta)$ are the stochastic joint model parameters which can be identified by using experimental results as described in the identification procedure in next section. $k_1(\theta)$ and $k_2(\theta)$ represent the equivalent linear stiffnesses of the slap and slip mechanisms in the contact interface, respectively. It is worth mentioning that $k_1(\theta)$ and $k_2(\theta)$ are the distribution of stiffness parameters over the contact interface and in the cases that several joint elements of the kind introduced in equation (2) are used to model the joint section, $k_1(\theta)$ and $k_2(\theta)$ are each governed by one random field for all elements.

The slip mechanism in the contact interface of the joint contributes to the energy dissipation in the structure. To consider this energy dissipation, the following damping matrix is proposed for the joint section,

$$[C_j]=\begin{bmatrix} 0 & 0 & 0 & 0 & 0 & 0 \\ 0 & 0 & 0 & 0 & 0 & 0 \\ 0 & 0 & c(\theta) & 0 & 0 & -c(\theta) \\ 0 & 0 & 0 & 0 & 0 & 0 \\ 0 & 0 & 0 & 0 & 0 & 0 \\ 0 & 0 & -c(\theta) & 0 & 0 & c(\theta) \end{bmatrix} \tag{3}$$

where $\mathrm{c}(\theta) = c_0(1 + \bar{\varepsilon}_3 f_3(\theta))$. c_0 and $0 < \bar{\varepsilon}_3 \ll 1$ are the mean values and deterministic constants and $f_3(\theta)$ is a zero mean random field describing the variability in the damping parameter of the joint element. The description given above about using several elements for modeling the joint section is applied to $c(\theta)$ as well.

Because of the overlap of the two substructures in the joint section, the mass effect of the joint section is twice the mass effect of the beam section which means $\left[M_j\right] = 2[M_b]$. By assembling the mass, damping and stiffness matrices of the beam and joint elements, finally the dynamic model governing the free vibration of the assembled structure shown in Figure 6 is obtained as,

$$[M]\{\ddot{q}\} + [C(\theta)]\{\dot{q}\} + [K(\theta)]\{q\} = \{0\} \tag{4}$$

where $[C(\theta)]$ and $[K(\theta)]$ contains the stochastic joint model parameters. In next section, the identification procedure for the joint model parameters is described.

Parameter identification procedure

Identification of the stochastic joint model parameters described in the previous section is considered by using experimental natural frequencies and employing the Bayesian identification approach as described in this section.

The natural frequencies of the assembled structure can be related to the joint element stiffness parameters by the following equation,

$$\mathbf{y} = \mathbf{f}(\boldsymbol{\theta}) \tag{5}$$

where $\boldsymbol{\theta}$, is the vector of joint element stiffness parameters, i.e. $\boldsymbol{\theta} = [k_1, k_2]^T$, $\mathbf{y} = [f_1, \dots, f_{\mathrm{m}}]^T$ is one set of measured natural frequencies (or observations) and $\mathbf{f}$ represents the mathematical model of the un-damped structure described by equation (4). Our goal is to identify the distribution of the joint element stiffness parameters, i.e. $k_1(\theta)$ and $k_2(\theta)$, by using the Bayesian identification approach provided that $\bar{N}$ sets of observation data (i.e. natural frequencies) are available.

Based on the Bayes' rule, the following equation governs the posterior probability of model parameters [38],

$$p(\boldsymbol{\theta}|\mathbf{y}) = \frac{p(\mathbf{y}|\boldsymbol{\theta})p(\boldsymbol{\theta})}{p(\mathbf{y})} \cong cp(\mathbf{y}|\boldsymbol{\theta})p(\boldsymbol{\theta}) \quad (6)$$

where $p(\boldsymbol{\theta})$ is the initial (prior) probability which includes any prior information about the joint element stiffness parameters and $p(\mathbf{y}|\boldsymbol{\theta})$ is the likelihood function which is the probability of having observed $\mathbf{y}$ given the joint element stiffness parameters $\boldsymbol{\theta}$. $p(\mathbf{y})$ is the probability of the observed data which is usually considered as a constant. Equation (6) describes the joint parameter distribution and the individual posteriors, i.e. $p(\theta_p|\mathbf{y})$, can be obtained by integrating equation (6) [39], where θ_p is one of the joint model parameters described in $\boldsymbol{\theta}$, i.e. $\theta_p = k_1$ or $\theta_p = k_2$. There is no closed form solution for such a posterior probability calculation and usually numerical methods are used to estimate $p(\theta_p|\mathbf{y})$.

Hasting [40] proposed the Monte Carlo Markov Chain (MCMC) algorithm for sampling the posterior probability by using equation (6). A good description about using MCMC algorithm in the context of structural dynamics can be found in [41]. The MCMC algorithm generates samples from the posterior probability of each parameter by constructing a Markov chain. The details of constructing Markov chains by using the Metropolis-Hasting algorithm ([40], [42]) and employing the Gibbs sampling approach is described in [43].

The main part of equation (6) is the likelihood function $p(\mathbf{y}|\boldsymbol{\theta})$. It is usually assumed in stochastic model updating that a Normal distribution describes the error function. This assumption limits the application of stochastic model updating since a good prior distribution for the parameters must be used to guarantee convergence. In this paper a new likelihood function is introduced which does not rely on the assumption of a Normal distribution for the error function.

The likelihood function $p(\mathbf{y}|\boldsymbol{\theta})$ in equation (6) is obtained in this paper as follows. For a given set of model parameters $\boldsymbol{\theta}$, the vector of natural frequencies $\bar{\mathbf{y}}$ is calculated by means of the system model $\mathbf{f}$. On the other side, since $\bar{N}$ sets of observation data are available, i.e. $\boldsymbol{Y} = [\mathbf{y}_{(1)} \quad \mathbf{y}_{(2)} \quad \cdots \quad \mathbf{y}_{(\bar{N})}]$, it is possible to estimate the distribution function (or statistical model) of each observed data- i.e. $\{g_i(.;\boldsymbol{\chi_i})|\boldsymbol{\chi_i} \in \mathrm{X}\}, i = 1,2,\dots,m$- using the method of maximum likelihood [44]. $\boldsymbol{\chi_i}$ denotes the vector of statistical model parameters which is obtained by maximizing the likelihood function $\mathcal{L}(\boldsymbol{\chi_i}, Y^i), i = 1,2,\dots,m$ where Y^i is the i$^{\text{th}}$ row of the observed data matrix $\boldsymbol{Y}$. As an example, for a Normal distribution $\boldsymbol{\chi_i} = [\sigma \quad \mu]^T$ and for a Beta distribution $\boldsymbol{\chi_i} = [a \quad b]^T$. The statistical parameter vector $\boldsymbol{\chi_i}$ is obtained such that,

$$\widehat{\boldsymbol{\chi}}_{\boldsymbol{i}} \in \{arg \max \Gamma;\ \boldsymbol{\chi_i} \in \mathrm{X}\} \tag{7}$$

where Γ can be either likelihood, log-likelihood or average log-likelihood functions. The statistical model fitted on some measured natural frequencies presented in Figure 4 are shown in Figure 7.

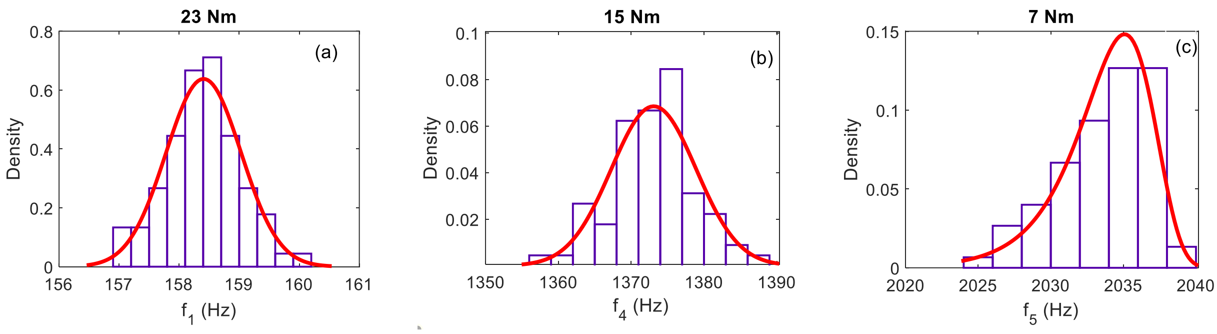

Figure 7. Fitted statistical models (solid lines) on measured natural frequencies (Bars): (a) 23Nm, Normal $= 158.4$, $\sigma = 0.625$, (b) 15Nm, Normal $\mu = 1373.1$, $\sigma = 5.827$, (c) 7Nm, Weibull, $A = 2035.08, B = 819.5$

After estimating the statistical model for each observed natural frequency, the likelihood function $p(\mathbf{y}|\boldsymbol{\theta})$ in equation (6) is calculated as,

$$p(\mathbf{y}|\boldsymbol{\theta}) = \prod_{\boldsymbol{i=1}}^{\boldsymbol{m}} g_i(\bar{y}_i; \boldsymbol{\chi_i}) \tag{8}$$

Identification of the joint model stiffness parameters are considered in the next section by using the method described in this section.

Identification results

Joint model stiffness parameters

To identify the distribution of the joint model stiffness parameters, the experimental natural frequencies presented in Figure 4 are used. First, an undamped dynamic model is constructed for the structure shown in Figure 1 by taking $[C(\theta)] = 0$ in equation (4). Timoshenko beam elements, as introduced in equations (1), are used to model the beam sections of the structure and the joint element of equation (2) is used to model the joint section. Overall, 50 beam elements and 5 joint elements are used. In the FE model the material properties of the beam sections are taken as $E = 208$ GPa and $\rho = 7860\ \mathrm{kg/m^3}$. Also the mass effects of the bolts and nuts, and the accelerometers are considered as point masses in the FE model with $m_b = 0.012$ kg and $I_b = 3.45 \times 10^{-6}\ \mathrm{kg.m^2}$ for the bolts and nuts and $m_b = 0.0075$ kg and $I_b = 9.84 \times 10^{-8}\ \mathrm{kg.m^2}$ for the accelerometers.

The Metropolis-Hasting algorithm is used to draw samples from the posterior function defined by equation (6) and hence to identify the distribution of joint element stiffness parameters $k_1(\theta)$ and $k_2(\theta)$ defined by equation (2). In this paper a Normal distribution function is considered to govern the initial probability of each joint element stiffness parameters, i.e. $\theta_p \sim \mathbf{N}(\mu_p, \sigma_p)$. Starting with an initial value for the joint element stiffness parameters vector $\boldsymbol{\theta}$, new random samples are generated by using the initial distribution function defined for each parameter, i.e. $\theta_p \sim \mathbf{N}(\mu_p, \sigma_p)$, and are accepted based on an accept-reject criterion. This procedure is continued until enough samples are generated and hence the distribution of joint element stiffness parameters are identified.

The mean value μ_p for the initial probability of each joint element stiffness parameter is estimated by updating a deterministic model using mean values of the first five natural frequencies, i.e. $\bar{f}_j, j = 1, \ldots, 5$. The deterministic model is obtained by choosing $k_i(\theta) = \bar{k}_i, i = 1,2$ in equation (2) and is updated by using the eigenvalue sensitivity approach [45]. The identified deterministic joint element stiffness parameters and the accuracy of the identified deterministic model are reported in Table 1 for the experimental results corresponding to a bolt tightening torque of 23 Nm.

Table 1. Updating of the deterministic model @ 23 Nm

	$\bar{f}_1$	$\bar{f}_2$	$\bar{f}_3$	$\bar{f}_4$	$\bar{f}_5$	$\bar{f}_6$	$\bar{f}_7$	$\bar{f}_8$
Exp.	158.41	442.81	860.93	1383.5	2045.7	2869.4	3438.9	4279.7
Updated	158.37	443.5	861.6	1382.7	2045.3	2809.0	3613.4	4172.2
Error (%)	-0.02	0.15	0.07	-0.06	-0.02	-2.10	5.07	-2.50

It is worth mentioning that the pressure distribution over the contact interface is non-uniform. Therefore ideally joint elements with different stiffness parameters should be used to model the joint section in the deterministic identification. However, increasing the number of unknown parameters could result in a badly conditioned problem which introduces difficulties in the identification procedure. Since identification of the deterministic model is mainly done to obtain an estimate for the mean value of the initial probability of each joint element stiffness parameter, the assumption of a constant distribution of bolt preload, which allows the modeling of the joint section using similar joint elements, is sufficient for this end.

In the identification procedure the mean values $\mu_p, p = 1,2$ and standard deviations $\sigma_p, p = 1,2$ of the initial PDFs are considered to be $\bar{k}_i$ and $\bar{k}_i/20$, $i = 1,2$, respectively. The identified deterministic joint element stiffness parameters for different bolt tightening torques are listed in Table 2.

Table 2. The identified deterministic joint element stiffness parameters

	7 Nm	15 Nm	23 Nm
$\bar{k}_1$	1690.2	1715.9	1763.2
$\bar{k}_2$	31047	34810	37402

The Metropolis-Hasting algorithm is run and 20k samples are generated from the posterior function described in equation (5) to identify the distribution of the joint model parameters. It is worth mentioning that the first 5k samples are neglected to ensure that the initial condition has no effects on the final results. The identified distributions for the joint element stiffness parameters are shown in Figure 8.

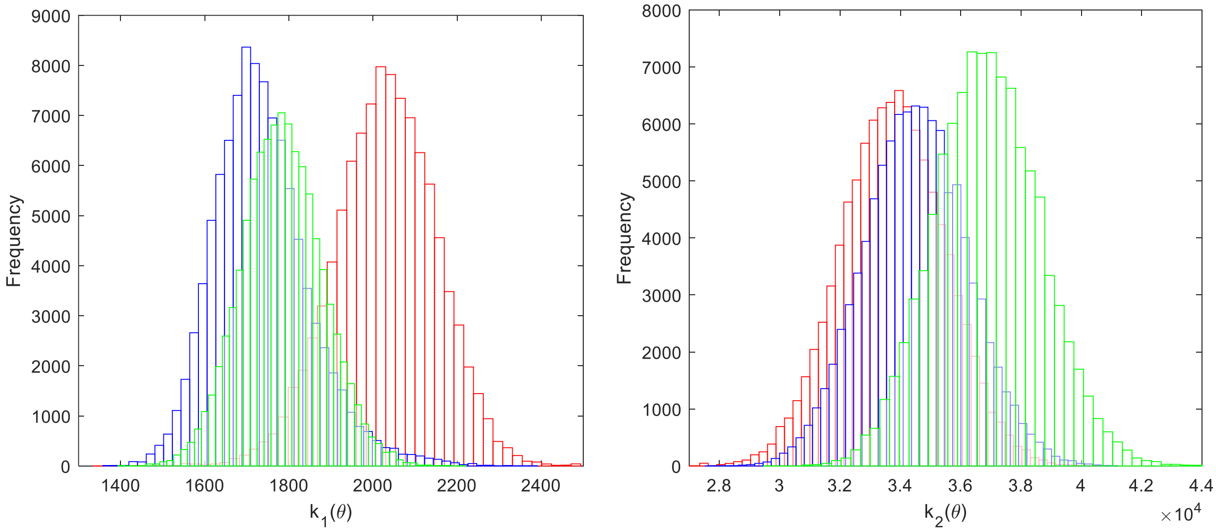

Figure 8. Identified distributions for the joint element stiffness parameters: 7 Nm (red), 15 Nm (blue) and 23 Nm (green)

Figure 8 shows that the identified joint model parameters follow a Normal distribution. In Figure 9 the correlation of the identified joint model parameters is shown. The two identified parameters are statistically independent representing independent contributions to the normal and tangent stiffnesses of the joint.

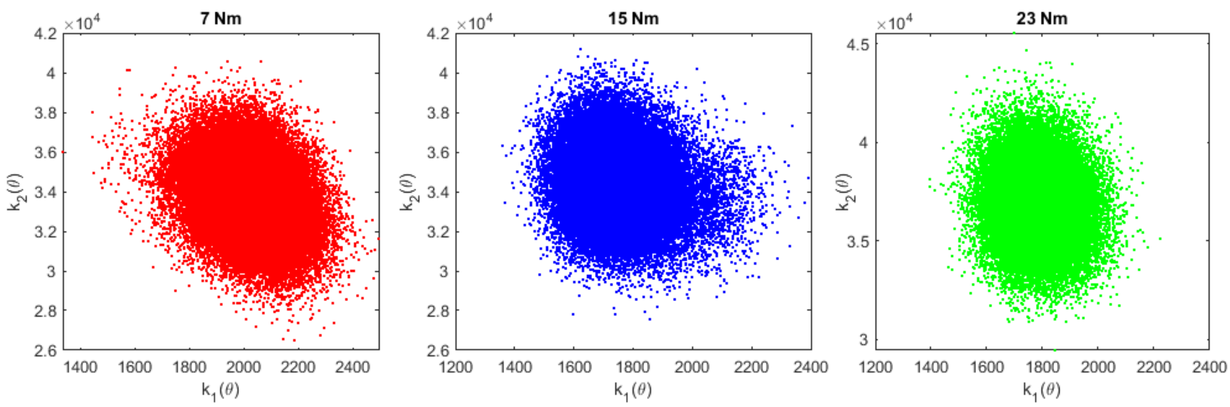

Figure 9. Correlation between the identified joint element stiffness parameters

The experimental natural frequencies are compared with the identified natural frequencies in Figures 10-12 for different bolt tightening torques.

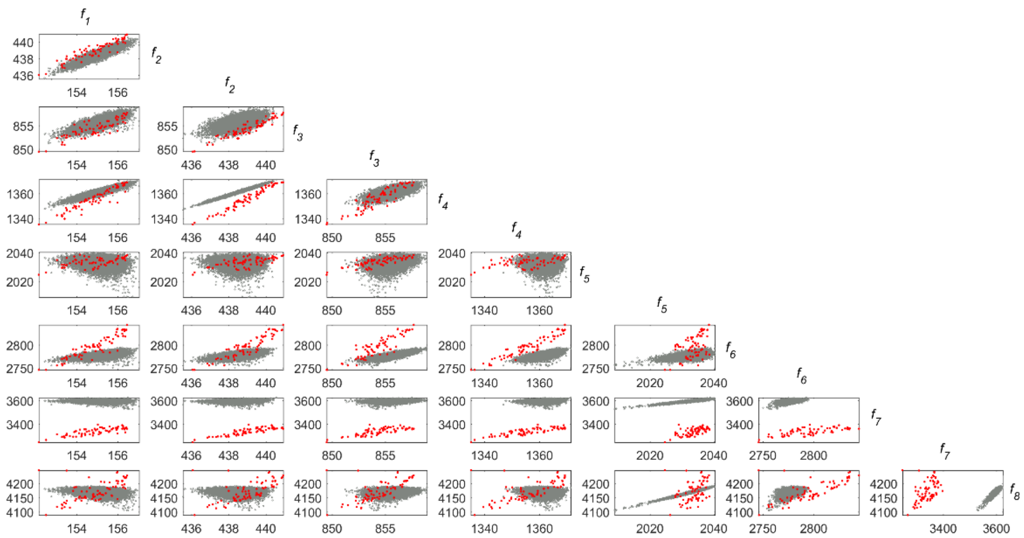

Figure 10. Experimental (red) vs. identified (grey) natural frequencies: 7 Nm

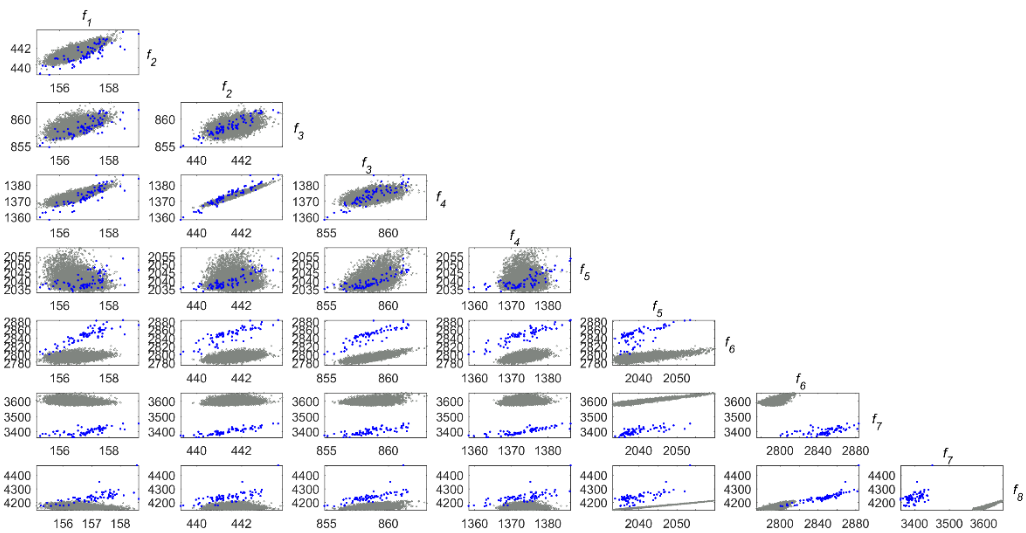

Figure 11. Experimental (blue) vs. identified (grey) natural frequencies: 15 Nm

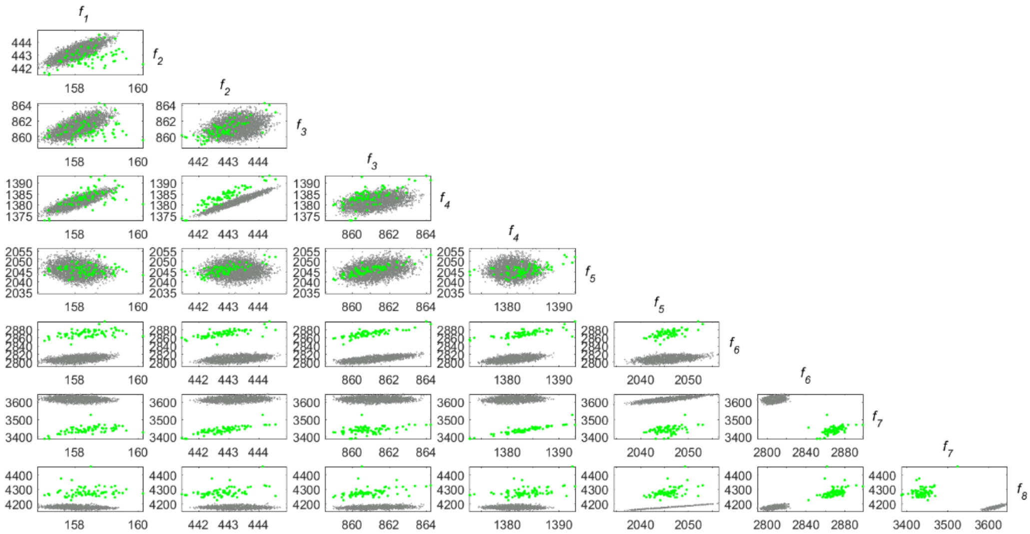

Figure 12. Experimental (green) vs. identified (grey) natural frequencies: 23 Nm

The results presented in Figures 10-12 show that the modeling approach and the identification procedure presented in this paper can effectively predict the experimental results for the frequencies that are used in the identification. Although the experimental data shows a higher correlation between natural frequencies, the proposed model can also predict the correlation that is consistent with the experimental results. In the other words, if the experimental results show a high correlation between two natural frequencies, then the model prediction also shows a high correlation between those frequencies. Another interesting observation is that although the updated mean values of the higher frequencies (modes 6, 7 and 8 which are not used for identification) have higher errors when compared to the identified lower frequencies, the scatter of predictions from the model have similar size and correlation with the scatter of experimental data. There are some outliers in the experimental results which is due to the possibility of exciting nonlinearities in the impact testing or due to other types of uncertainties. Excitation of nonlinearities is more likely in the higher modes and this is one reason for the poor prediction of the proposed linear model for the higher modes. The other key aspect is that these higher modes could induced different local deformations in the joints, and hence different physical phenomena might be excited in the joints.

Joint model damping parameter

As it was explained in the previous sections, the variability in the experimental damping ratios presented in Figure 5 is not as significant as the variability in the experimental natural frequencies. Also, due to the nature of damping extraction approaches, the existing variability cannot be attributed only to the variability in the contact interface parameters and a part of this variability is due to the error in damping ratio extraction from experimentally measured FRFs. Therefore, the experimental results presented in Figure 5 are not suitable for quantification of uncertainty in the damping parameter of the joint element. Instead, the mean values of experimental damping ratios presented in Figure 5 are a good measure of the overall contribution of the damping in the contact interface to the damping of different modes of the structure. The mean values of the experimental damping ratios are used in this section to identify a deterministic damping model for the joint section of the structure as follows.

A deterministic model is constructed for the structure by considering $c(\theta) = \bar{c}$, $k_1(\theta) = \bar{k}_1$ and $k_2(\theta) = \bar{k}_2$ in equation (4). $\bar{k}_1$ and $\bar{k}_2$ are identified by using mean values of the measured natural frequencies and employing the eigenvalue sensitivity approach as described in the previous sections. $\bar{c}$ is identified by comparing the mean values of the first five experimental damping ratios presented in Figure 5 with their counterparts from the analytical model which are obtained from the eigenvalues of matrix $[A]$, where [46]

$$[A] = \begin{bmatrix} [0] & [I] \\ -[M]^{-1}[K] & -[M]^{-1}[C] \end{bmatrix} \tag{9}$$

Comparison between experimental and identified FRFs and the corresponding identified damping coefficient of the joint element are shown in Figure 13.

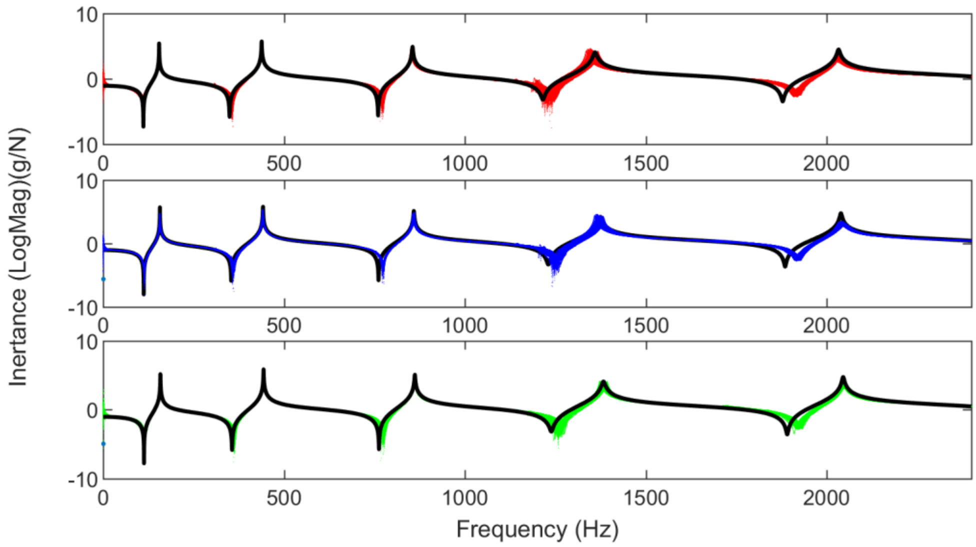

Figure 13. Comparison between the experimental and identified FRFs: 7 Nm (red) $\bar{c} = 0.14$ Ns/m, 15 Nm (blue) $\bar{c} = 0.12$ Ns/m, 23 Nm (green) $\bar{c} = 0.15$ Ns/m

The results presented in Figure 13 show that the damping matrix of equation (3) is capable of accurately representing the damping in the contact interface.

The mean values of the experimental damping ratios for the first five modes are shown in Figure 14:

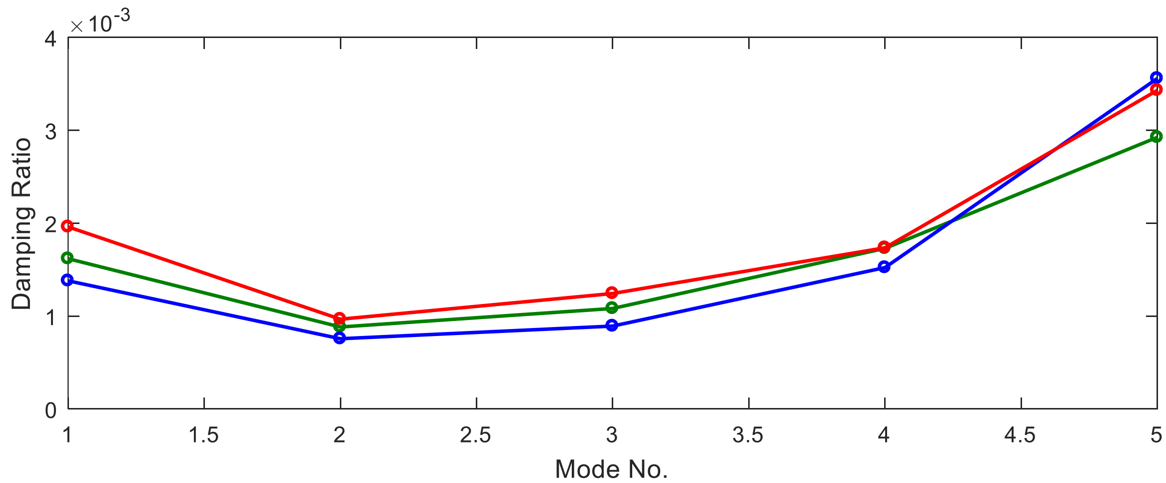

Figure 14- mean values of the experimental damping ratios: 7 Nm (red), 15 Nm (blue), 23 Nm (green).

Figure 14 shows that by increasing the mode number, the damping ratio, which is a measure of the amount of energy dissipated in the contact interface in each mode, initially decreases and then increases. Energy dissipation in assembled structures takes place in the joint contact interfaces mainly by a micro-slip mechanism. To determine the connection between the damping ratio of each mode and the position of the contact interface in the structure, the mode shapes of the identified deterministic finite element model are shown in figure 15,

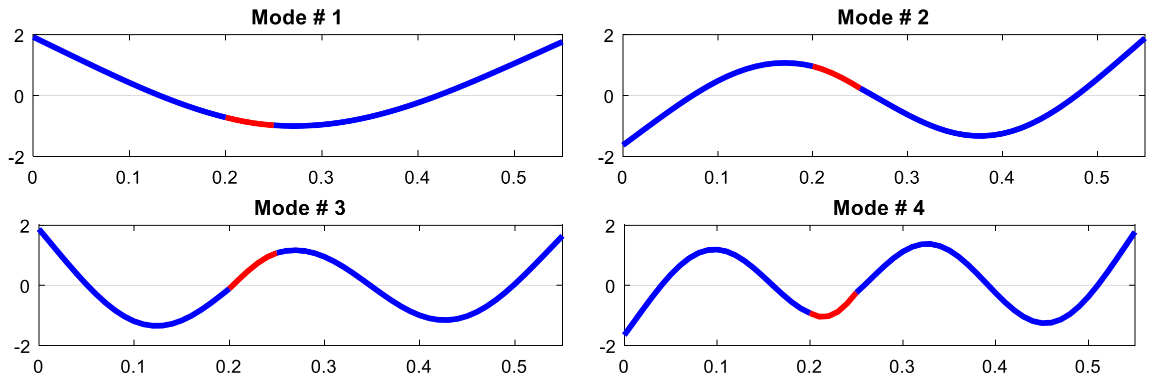

Figure 15- Mode shapes of the identified deterministic model (@ 23 N.m): beam sections (blue) and joint section (red)

Figure 15 indicates that the curvature of the beam is smaller for modes 2 and 3 which results in a lower energy dissipation in the contact interface.

Conclusions

In this paper an experimental investigation of the effects of variability in the surface roughness quality and bolt preload on the variability of modal parameters of assembled structures was considered. Experimental results show that there is a significant variability in the natural frequencies while variability in the damping ratios is much less than for the natural frequencies. A dynamic model was then constructed for the assembled structure in which the joint section was modeled using stochastic generic joint elements. A new likelihood function was proposed and the distribution of the stiffness parameters of the joint element was identified by using experimental natural frequencies and employing a Bayesian identification approach using the proposed likelihood function. The identified results showed a good agreement with experimental results for the lower modes used in the identification.

The reason for the poor prediction of experimental higher modes by the proposed linear joint model can be attributed to the excitation of nonlinearities in the contact interface which is more likely in higher modes. Finally, a deterministic damping model was identified for the contact interface by using the mean values of the experimental damping ratios.

Acknowledgment

This research is funded by the Engineering and Physical Sciences Research Council through Grant no. EP/P01271X/1. Hadi Madinei acknowledges the financial support from the Impact Acceleration Account grant (IAA2017) for carrying out the experiments presented in this article.

Appendix

The mass matrix of Timoshenko beam element is given by,

$$[M_b] = \rho AL \begin{bmatrix} 1/3 & 0 & 0 & 1/6 & 0 & 0 \\ 0 & A_1 & C_1 & 0 & B_1 & -D_1 \\ 0 & C_1 & E_1 & 0 & D_1 & -F_1 \\ 1/6 & 0 & 0 & 1/3 & 0 & 0 \\ 0 & B_1 & D_1 & 0 & A_1 & -C_1 \\ 0 & -D_1 & -F_1 & 0 & -C_1 & E_1 \end{bmatrix} \quad \text{(A1)}$$

$$A_1 = \left(\frac{13}{35} + \frac{7}{10}\phi + \frac{1}{3}\phi^2 + \frac{6}{5}\left(\frac{r}{L}\right)^2\right)/(1+\phi)^2 \quad \text{(A2)}$$

$$B_1 = \left(\frac{9}{70} + \frac{3}{10}\phi + \frac{1}{6}\phi^2 - \frac{6}{5}\left(\frac{r}{L}\right)^2\right)/(1+\phi)^2 \quad \text{(A3)}$$

$$C_1 = L\left(\frac{11}{210} + \frac{11}{120}\phi + \frac{1}{24}\phi^2 + \left(\frac{1}{10} - \frac{1}{2}\phi\right)\left(\frac{r}{L}\right)^2\right)/(1+\phi)^2 \quad \text{(A4)}$$

$$D_1 = L\left(\frac{13}{420} + \frac{3}{40}\phi + \frac{1}{24}\phi^2 - \left(\frac{1}{10} - \frac{1}{2}\phi\right)\left(\frac{r}{L}\right)^2\right)/(1+\phi)^2 \quad \text{(A5)}$$

$$E_1 = L^2\left(\frac{1}{150} + \frac{1}{60}\phi + \frac{1}{120}\phi^2 + \left(\frac{2}{15} + \frac{1}{6}\phi + \frac{1}{3}\phi^2\right)\left(\frac{r}{L}\right)^2\right)/(1+\phi)^2 \quad \text{(A6)}$$

$$F_1 = L^2\left(\frac{1}{140} + \frac{1}{60}\phi + \frac{1}{120}\phi^2 + \left(\frac{1}{30} + \frac{1}{6}\phi - \frac{1}{6}\phi^2\right)\left(\frac{r}{L}\right)^2\right)/(1+\phi)^2 \quad \text{(A7)}$$

where $r = \sqrt{I/A}$ is the radius of gyration of the cross section.

1 References

[1] D. J. Segalman, D. L. Gregory, M. J. Starr, B. R. Resor, M. D. Jew, J. P. Lauffer and N. M. Ames, "Handbook on Dynamics of Jointed Structures," Sandia National Laboratories, Albuquerque, 2009.

[2] R. A. Ibrahim and C. L. Pettit, "Uncertainties and dynamic problems of bolted joints and other fasteners," *Journal of Sound and Vibration,* vol. 279, no. 3-5, pp. 857-936, 2005.

[3] M. R. Brake, P. Reuss, D. J. Segalman and L. Gaul, "Variability and Repeatability of Jointed Structures with Frictional Interfaces," in *International Modal Analysis Conference*, Orlando, 2014.

[4] S. N. Gangadharan, E. Nikolaidis and R. Haftka, " Probabilistic system identification of two flexible joint models," *AIAA Journal,* vol. 29, no. 8, pp. 1319-1326, 1991.

[5] C. Lopez, A. Baldomir, E. Menga, S. Hernandez, C. Cid and D. Freire, "A study of uncertainties in dynamic properties of assembled aircraft structures," in *in International Conference on Noise and Vibration Engineering - International Conference on Uncertainty in Structural Dynamics ISMA2016-USD2016*, Leuven, Belgium, 2016.

[6] Q. T. Guo and L. M. Zhang, "Identification of the Mechanical Joint Parameters with Model Uncertainty," *Chinese Journal of Aeronautics,* vol. 18, no. 1, pp. 47-52, 2005.

[7] G. M. Castelluccio and M. R. W. Brake, "On the origin of computational model sensitivity, error, and uncertainty in threaded fasteners," *Computers and Structures,* vol. 186, pp. 1-10, 2017.

[8] H. H. Khodaparast, J. E. Mottershead and M. I. Friswell, "Perturbation methods for the estimation of parameter variability in stochastic model updating," *Mechanical systems and signal processing,* vol. 22, no. 8, pp. 1751-1773, 2008.

[9] S. E. Fang, Q. H. Zhang and W. X. Ren, "An interval model updating strategy using interval response surface models," *Mechanical Systems and Signal Processing,* vol. 60, pp. 909-927, 2015.

[10] M. Faes, M. Broggi, E. Patelli, Y. Govers, J. E. Mottershead, M. Beer and D. Moens, "A multivariate interval approach for inverse uncertainty quantification with limited experimental data," *Mechanical Systems and Signal Processing,* vol. 118, pp. 534-548, 2019.

[11] Y. S. Erdogan and P. G. Bakir, "Inverse propagation of uncertainties in finite element model updating through use of fuzzy arithmetic," *Engineering Applications of Artificial Intelligence,* vol. 26, no. 1, pp. 357-367, 2013.

[12] A. Hanselowski, S. Ihrle and M. Hanss, "A fuzzy model updating technique motivated by Bayesian inference," in *. Proc. of the 1st International Conference on Uncertainty Quantification in Computational Sciences and Engineering – UNCECOMP*, Crete Island, Greece, 2015.

[13] H. Haddad Khodaparast, Y. Govers, I. Dayyani, S. Adhikari, M. Link, M. I. Friswell and J. Sienz, "(2017). Fuzzy finite element model updating of the DLR AIRMOD test structure," *Applied Mathematical Modelling,* vol. 52, pp. 512-526, 2017.

[14] H. Haddad Khodaparast, J. E. Mottershead and M. I. Friswell, "Perturbation methods for the estimation of parameter variability in stochastic model updating," *Mechanical systems and signal processing,* vol. 22, no. 8, pp. 1751-1773, 2008.

[15] Y. Govers and M. Link, "Stochastic model updating—covariance matrix adjustment from uncertain experimental modal data.," *Mechanical Systems and Signal Processing,* vol. 24, no. 3, pp. 696-706, 2010.

[16] T. A. Silva, N. M. Maia, L. M. and J. E. Mottershead, "Parameter selection and covariance updating," *Mechanical Systems and Signal Processing,* vol. 70, pp. 269-283, 2016.

[17] X. G. Hua, Y. Q. Ni, Z. Q. Chen and J. M. Ko, " An improved perturbation method for stochastic finite element model updating," *International Journal of Numerical Methods in Engineering,* vol. 73, no. 13, pp. 1845-1864, 2008.

[18] I. Behmanesh, B. Moaveni, G. Lombaert and C. Papadimitriou, "Hierarchical Bayesian model updating for structural identification," *Mechanical Systems and Signal Processing,* vol. 64, pp. 360-376, 2015.

[19] E. Patelli, Y. Govers, M. Broggi, H. M. Gomes, M. Link and J. E. Mottershead, "Sensitivity or Bayesian model updating: a comparison of techniques using the DLR AIRMOD test data," *Archive of Applied Mechanics,* vol. 87, no. 5, pp. 905-925, 2017.

[20] A. B. Abdessalem, N. Dervilis, D. Wagg and K. Worden, "An Efficient Likelihood-Free Bayesian Computation for Model Selection and Parameter Estimation Applied to Structural Dynamics," *Structural Health Monitoring, Photogrammetry & DIC,* vol. 6, 2019.

[21] Y. Govers, H. H. Khodaparast, L. M. and J. E. Mottershead, "A comparison of two stochastic model updating methods using the DLR AIRMOD test structure," *Mechanical Systems and Signal Processing,* vol. 52, pp. 105-114, 2015.

[22] E. Simoen, G. De Roeck and G. Lombaert, "Dealing with uncertainty in model updating for damage assessment: A review," *Mechanical Systems and Signal Processing,* vol. 56, pp. 123-149, 2015.

[23] H. Ahmadian and H. Jalali, "Identification of bolted lap joints parameters in assembled structures," *Mechanical Systems and Signal Processing,* vol. 21, no. 2, pp. 1041-1050, 2007.

[24] R. A. Onions and J. F. Archard, "The contact of surfaces having a random structure," *Journal of Applied Physics,* vol. 6, pp. 289-304, 1973.

[25] H. A. Sherif and S. S. Kosa, "Relationship between normal and tangential contact stiffness of nominally flat surfaces," *Wear,* vol. 151, pp. 49-62, 1991.

[26] M. L. Raffa, F. Lebon and G. Vairo, "Normal and tangential stiffnesses of rough surfaces in contact via an imperfect interface model," *International Journal of Solids and Structures,* vol. 87, pp. 245-253, 2016.

[27] D. J. Ewins, Modal Testing: Theory, Practice and Application, Hertfordshire: Research Studies Press LTD, 2000.

[28] S. M. Han, H. Benaroya and T. Wei, "Dynamics of transversely vibrating beams using four engineering theories," *Journal of Sound and Vibration,* vol. 255, no. 5, pp. 935-988, 1999.

[29] F. Adel, S. Shokrollahi, M. J. Omidi and H. Ahmadian, "A model updating method for hybrid composite/aluminum bolted joints using modal test data," *Journal of Sound and Vibration,* vol. 396, pp. 172-185, 2017.

[30] S. Bograd, P. Reuss, A. Schmidt, L. Gaul and M. Mayer, "Modeling the dynamics of mechanical joints," *Mechanical Systems and Signal Processing,* vol. 25, no. 8, pp. 2801-2826, 2011.

[31] H. Jalali, "Linear contact interface parameter identification using dynamic characteristic equation," *Mechanical Systems and Signal Processing,* Vols. 66-67, p. 111–119, 2016 .

[32] M. H. Mayer and L. Gaul, "Segment-to-segment contact elements for modelling joint interfaces in finite element analysis," *Mechanical Systems and Signal Processing,* vol. 21, no. 2, pp. 724-734, 2007.

[33] H. Ahmadian and H. Jalali, "Generic element formulation for modelling bolted lap joints," *Mechanical Systems and Signal Processing,* vol. 21, no. 5, pp. 2318-2334, 2007.

[34] H. Jalali, H. Ahmadian and M. J. E, "Identification of nonlinear bolted lap-joint parameters by force-state mapping," *International Journal of Solids and Structures,* vol. 44, p. 8087–8105, 2007.

[35] L. Gaul and J. Lenze, " Nonlinear dynamics of structures assembled by bolted joints," *Acta Mechanica ,* vol. 125, pp. 169-181, 1997.

[36] K. Lingfei, J. Heling, A. H. Ghasemi and L. Yan, "Condensation modeling of the bolted joint structure with the effect of nonlinear dynamics," *Journal of Sound and Vibration,* vol. 442, pp. 657-676, 2019.

[37] "An offset finite element model and its application in predicting sheet metal assembly variation," *International Journal of Machine Tools and Manufacture,* vol. 35, no. 11, pp. 1545-1557, 1995.

[38] T. Bayes, "An Essay towards solving a Problem in the Doctrine of Chances," *Philosophical Transactions of the Royal Society of London,* vol. 53, p. 370–418, 1763.

[39] G. C. Tiao and A. Zellner, "Bayes's theorem and the use of prior knowledge in regression analysis," *Biometrika,* vol. 51, no. 1/2, p. 219–230, 1964.

[40] W. K. Hastings, "Monte Carlo sampling methods using Markov chains and their applications," *Biometrika,* vol. 57, no. 1, pp. 97-109, 1970.

[41] J. M. Nichols, W. A. Link, K. D. Murphy and C. C. Olson, "A Bayesian approach to identifying structural nonlinearity using free-decay response: application to damage detection in composites," *Journal of Sound and Vibration,* vol. 329, no. 15, p. 2995–3007, 2010.

[42] N. Metropolis, A. W. Rosenbluth, M. N. Rosenbluth, A. H. Teller and E. Teller, "Equation of state calculations by fast computing machines," *The Journal of Chemical Physics,* vol. 21, no. 6, p. 1087–1092, 1953.

[43] J. M. Nichols, E. Z. Moore and K. D. Murphy, "Bayesian identification of a cracked plate using a population-based Markov Chain Monte Carlo method," *Computers and Structures ,* vol. 89, p. 1323–1332, 2011.

[44] A. P. Dempster, L. M. Laird and D. B. Rubin, "Maximum-likelihood from incomplete data via the EM algorithm," *Journal of the Royal Statistical Society Series B,* vol. 39, pp. 1-38, 1977.

[45] J. E. Mottershead and M. I. Friswell, Finite element model updating in structural dynamics, Netherlands: Kluwer Academic Publishers, 1995.

[46] L. Meirovitch, Elements of Vibration Analysis, New York: McGraw-Hill, 1986.